Asociación Argentina
de Mecánica Computacional

Mecánica Computacional Vol XXVII, págs. 3367-3380 (artículo completo)
Alberto Cardona, Mario Storti, Carlos Zuppa. (Eds.)
San Luis, Argentina, 10-13 Noviembre 2008

GENERALIZED NUMERICAL MODEL FOR THE SIMULATION OF ELECTROPHORETIC METHODS IN MICROFLUIDIC CHIPS

Pablo A. Kler[a], Fabio A. Guarnieri[a,b] and Claudio L. A. Berli[c,d]

[a]*CIMEC, INTEC (UNL-CONICET), PTLC, El Pozo, 3000, Santa Fe, Argentina.*
[b]*Fac. de Bioingeniería, UNER, 3100, Oro Verde, Argentina.*
[c]*INTEC (UNL-CONICET), Güemes 3450, 3000, Santa Fe, Argentina.*
[d]*Dpto. Física, FBCB, UNL, Ciudad Universitaria, 3000, Santa Fe, Argentina.*

Keywords: Microfluidic chips, Electrophoresis, Numerical model, PETSC-FEM.

Abstract. Electrophoretic methods are separation techniques based on the mobility of ions under the action of an external electric field. These techniques, which are widely used in chemical and biochemical analysis, have been miniaturized in the last years and now represent one of the most important applications of the lab-on-a-chip technology. In this work, a generalized numerical model of electrophoresis on microfluidic devices is presented. The model is based on the set of equations that governs electrical phenomena (Poisson equation), fluid dynamics (Navier-Stokes equations), mass transport (Nerst-Planck equation) and chemical reactions. The model is said to be generalized because it covers different techniques such as capillary eletrophoresis and isoelectric focusing, and allows to simulate processes involving multiple analytes and complex electrolytes buffers. Moreover, the relationship between the buffer characteristics (ionic strength, pH) and physicochemical properties of channel walls is taken into consideration. The numerical simulation is carried out by using PETSC-FEM (Portable, Extensible Toolkit for Scientific Computation - Finite Elements Method), in a Python environment developed at CIMEC using high performance parallel computing and solving techniques based on domain decomposition methods. Finally, examples of interest involving electrophoresis on chips are considered as study cases.

1 INTRODUCTION

Electrophoretic methods are separation techniques based on the mobility of ions under the action of an external electric field. These techniques, which are widely used in chemical and biochemical analysis, have been miniaturized in the last years and now represent one of the most important applications of the microscale total analysis systems (μTAS) technology (Manz et al., 1990). The benefits of μTAS are a reduction of consumption of samples and reagents, shorter analysis times, greater sensitivity, portability and disposability (Reyes, 2002). Microscopic channels are defined by using materials and fabrication methods that were adopted from the developed microelectronics industry (Koch et al., 2000). Computational and analytical simulation of on-chip processes serve to reduce the time from concept to chip (Erickson, 2005). However, there are difficulties due to the several orders of magnitude of the relevant length scales involved: the electric double layer (EDL) thickness (in nm), microchannels width (in μm), and microchannels length (in mm). At the same time, the most challenging and interesting aspect of computational simulation of microfluidic chips is the multiphysics nature, which combines fluidics, mass transport, thermal, mechanics, electronics and reaction kinetics.

The earliest mathematical models for electrophoresis were developed by Saville et al. (1986) and Palusinski et al. (1986). These one dimensional models are valid for monovalent analytes in a stagnant electrolyte solution (without electroosmotic flow). Some of the first numerical simulations of fluid flow and species transport for microfluidic chips were addressed to electrokinetic focusing and sample dispensing techniques (Patankar et al.,1998; Ermakov et al., 1998; 2000),and they employed an algorithm based on finite volume method in a structured grid. Bianchi et al. (2000) performed 2D finite element simulations artificially increasing the EDL thickness. Arnaud et al. (2002) developed a finite element simulation of isoelectric focusing for ten species, without considering migration nor convection. Chatterjee (2003) developed a 3D finite volume model to study several applications in microfluidics. More recently, Kler et al. (2006) developed a 3D FEM model to describe the transport of non-charged species by electroosmotic flow (EOF), and Barz et al. (2007) developed a fully-coupled modeling for electrokinetic flow in microfluidic devices employing 2D finite elements.

In this paper, a generalized numerical model for electrophoretic processes in microfluidic chips is presented. The model is based on the set of coupled equations that governs flow field, electric field, mass transport and chemical reactions. The relationship between the buffer pH and the electric potential of channel walls is taken into consideration (numerical simulations with this kind of coupling were not reported before). The numerical simulation is carried out by using high performance parallel computing (Kler et al., 2007; Dalcín et al., 2008) and solving techniques based on domain decomposition methods.

2 MODELLING

In this section a mathematical model to simulate 3D and time-dependent electrophoretic phenomena in microdevices is presented. The model can also work in 1D and 2D domains, or stationary mode. In what follows, first the fuid mechanics and the basis of electroosmotic flow is discussed, then the mass transport balance for all species considered and the chemistry involved is presented.

2.1 Flow field

In the framework of continuum fluid mechanics, fluid velocity (u) and pressure (p) are governed by the following set of coupled equations (Saville et al., 1986; Probstein, 1989; Li, 2004):

$$\frac{\partial \rho}{\partial t} + \underline{\nabla} \cdot (\rho \underline{u}) = 0 \tag{1}$$

$$\rho \left(\frac{\partial \underline{u}}{\partial t} + \underline{u} \cdot \underline{\nabla} \underline{u} \right) = -\underline{\nabla} p + \mu \nabla^2 \underline{u} + \rho \underline{g} - \rho_e \underline{\nabla} \phi \tag{2}$$

Equation (1) expresses the conservation of mass for fluids. Equation (2) (Navier-Stokes equation) expresses the conservation of momentum for Newtonian fluids of viscosity μ and density ρ, subjected to gravitational field of acceleration g and electric potential ϕ . The last term on the RHS of equation (2) represents the contribution of electrical forces to the momentum balance, where $\rho_e = e \sum_j z_j c_j$ is the electric charge density of the electrolyte solution, obtained as the summation over all type-j ions, with ionic valence z_j and concentration c_j, e is the elementary charge. In the fluid bulk, charge density tends to zero, thus an approximation to reduce the effects of electric forces nearby the channel wall can be used, this is called thin double layer approximation.

2.2 Thin EDL approximation

The thickness of the EDL is quantified through Debye length (Probstein, 1989; Hunter, 1992),

$$\lambda = \left(\frac{e^2}{\epsilon k_B T} \sum_{j=0}^{N} z_i c_i^{(b)} \right)^{-\frac{1}{2}} \tag{3}$$

where $c_j^{(b)}$ is the bulk concentration of ions, ϵ is the electric permittivity, k_B is Boltzmann constant and T is the absolute temperature. For the ionic concentrations normally used in practice, $\lambda \approx$ 1-10 nm, while cross-sectional channel dimensions are 10-100 μm. Consequently, $\rho_e \approx 0$ in most of the flow domain, except in the close vicinity of charged interfaces. When an external electric field $\underline{\nabla} \phi_a$ is applied tangent to the interface, the electric forces acting on excess ions in the EDL drag the surrounding liquid, and thus EOF develops. For thin EDL in relation to the channel width (h), the effect is confined to a certain plane parallel to the channel wall, also designated shear plane, where the surface potential is the electrokinetic potential (ζ). Under these conditions, the electro-osmotically driven flow can be regarded as the result of an electrically-induced 'slip velocity', the magnitude of which is (Probstein, 1989; Hunter, 1992):

$$\underline{u}_{EO} = -\frac{\epsilon \zeta}{\mu} \underline{\nabla} \phi_a \tag{4}$$

Due to the fact that $\rho_e = 0$, ϕ_a can be calculated from Laplace's equation:

$$\nabla^2 \phi_a = 0 \tag{5}$$

Further, the last term on the RHS of equation (2) vanishes, and the EOF is considered by using $\underline{u}_{EO}$ as a boundary value at channel walls. This approximation is valid for large values of h/λ, which is usually the case in micro-scale channels at moderate ionic concentrations.

2.3 Electrokinetic potential as a function of the electrolyte composition

The electrokinetic potential at the solid-fluid interface depends on the charge generation mechanism of the surface. In principle, it may be thought that solid walls expose toward the fluid a certain number of specific sites (n_S) able to release or take H^+ ions, with a dissociation constant K_S. In equilibrium with an aqueous electrolyte solution, the surface becomes electrically charged. For the case of interfaces containing weak acid groups, such as silanol in fused silica capillaries and carboxyl in synthetic polymer materials, the following relationship is appropriate (Berli et al., 2003):

$$\left(8\epsilon k_B T c^{(b)}\right)^{(1/2)} \sinh\left(\frac{z e \zeta}{2 k_B T}\right) = \frac{-e n_s}{1+10^{(pK_s - pH)} e^{-e\zeta/k_B T}} \tag{6}$$

Therefore, if the parameters that characterize the interface are known (n_S, K_S), the ζ-potential can be readily predicted for different values of pH and ion concentrations $c^{(b)}$. Then the electro-osmotic velocity is directly coupled to the electrolyte composition. Empirical formulas were also reported in order to simplify calculations (Kirby et al., 2004).

2.4 Electric potential

Equation (5) is the simplest way to obtain the electric potential field in the flow domain. Nevertheless, this equation does not take into account possible variations of the electric field due to ion distributions. In order to consider (local) non-zero charge density due to buffer constituents or sample concentrations in the fluid, the equation (7) is introduced.

$$\underline{\nabla} \cdot \underline{i} = 0 \tag{7}$$

where $\underline{i}$ is the electric current density. Specifically, the current density is given by the sum of different fluxes of charged species:

$$\underline{i} = F \sum_{j=1}^{N} z_j \underline{j}_j \tag{8}$$

where $\underline{j}_j$ is the molar flux of the j-specie, established by the Nerst – Plank equation:

$$\underline{j}_j = -\Omega_j z_j F c_j \underline{\nabla} \phi - D_j \underline{\nabla} c_j + c_j \underline{u} \tag{9}$$

In equation (9) Ω_j and D_j are the ion mobility and diffusivity respectively. Finally by combining equations (7), (8), and (9) equation (10) is obtained.

$$\underline{\nabla} . \left(-F^2 \sum_{j=1}^{N} z_j^2 \Omega_j c_j \underline{\nabla} \phi - F \sum_{j=1}^{N} z_j D_j \underline{\nabla} c_j + F \sum_{j=1}^{N} \underline{u} z_j c_j\right) = 0 \tag{10}$$

which enable us to solve the electric potential. It should be noted here that ϕ is the total potential, which is regarded as the superposition of the applied potential ϕ_a and the one generated by local variation of concentrations species.

2.5 Mass transport and chemistry

The mass transport of weakly concentrated sample ions and buffer electrolyte constituents

can be modeled by a linear superposition of migrative, convective and diffusive transport mechanisms and a reactive term. In a non-stationary mode, for the j-type specie, this is:

$$\frac{\partial c_j}{\partial t}+\nabla\cdot(-z_j\Omega_j\nabla\phi\cdot c_j+\underline{u}\cdot c_j-D_j\nabla c_j)-r_j=0 \tag{11}$$

Following the chemistry problem is described and an expression for r_j is defined. Different components, weak electrolyte analytes and buffer components (acids, bases and ampholytes), strong analytes, and the hydrogen ion particularly have to be considered. In electrolyte chemistry the processes of association and dissociation are much faster than the transport electrokinetic processes, hence, it appears to be a good approximation to adopt chemical equilibrium constants to model the reactions present in our problem. In this sense, the strong electrolytes are considered as completely dissociated, this equilibrium relations were not included in the mathematical model.

Acids

The dissociation reaction is,

$$AH \underset{k_k}{\overset{k_{ij}}{\Leftrightarrow}} A^- + H^+ \tag{12}$$

then the equilibrium state is caracterized by,

$$\frac{k_{ij}}{k_k}=\frac{[AH]}{[A^-][H^+]}=k_a^{-1}=10^{pk_a} \tag{13}$$

where the square brackets represents molar concentration of the specie:

$$[AH]=c_{AH} \tag{14}$$

and

$$pK_a=-\log_{10}K_a \tag{15}$$

Then the expression of r_j is obtained for the disociated acid,

$$r_{[A^-]}=-k_{ij}[A^-][H^+]+k_k[AH] \tag{16}$$

for the non-disociated acid,

$$r_{[AH]}=k_{ij}[A^-][H^+]-k_k[AH] \tag{17}$$

and for hydrogen ion,

$$r_{[H^+]}=-k_{ij}[A^-][H^+]+k_k[AH] \tag{18}$$

Bases

The dissociation reaction is,

$$BH^+ \underset{k_k}{\overset{k_{ij}}{\Leftrightarrow}} B + H^+ \tag{19}$$

then the equilibrium state is caracterized by,

$$\frac{k_{ij}}{k_k} = \frac{[BH^+]}{[B][H^+]} = k_b^{-1} = 10^{pk_b} \tag{20}$$

Then the expression of r_j is obtained for the disociated base,

$$r_{[BH^+]} = k_{ij}[B][H^+] - k_k[BH^+] \tag{21}$$

for the non-disociated base,

$$r_{[B]} = -[B][H^+] + k_k[BH^+] \tag{22}$$

and for hydrogen ion,

$$r_{[H^+]} = -k_{ij}[B][H^+] + k_k[BH^+] \tag{23}$$

Ampholythes

Two reactions are considered:

$$PH \underset{k_k}{\overset{k_{ij}}{\Leftrightarrow}} P^- + H^+ \tag{24}$$

$$PH_2^+ \underset{k_n}{\overset{k_{lm}}{\Leftrightarrow}} PH + H^+ \tag{25}$$

Then, combining the previous sets of equations equation (26) is obtained.

$$r_{[P^-]} = -k_{ij}[P^-][H^+] + k_k[PH] \tag{26}$$

$$r_{[PH]} = k_{ij}[P^-][H^+] - k_k[PH] - k_{lm}[PH][H^+] + k_n[PH_2^+] \tag{27}$$

$$r_{[PH_2^+]} = k_{lm}[PH][H^+] - k_n[PH_2^+] \tag{28}$$

$$r_{[H^+]} = -k_{ij}[P^-][H^+] + k_k[PH] - k_{lm}[PH][H^+] + k_n[PH_2^+] \tag{29}$$

3 SIMULATION METHODOLOGY

In order to solve the entire problem four equations need to be considered: equation (10) to obtain electric potential, equations (1) and (2) to obtain velocity and pressure fields, and finally equation (11) to obtain concentration fields.

3.1 Charge conservation equation

Equation (10) was solved in a stationary mode, then it is not necessary to set initial conditions nor time stepping settings

Boundary conditions

Boundary conditions for the electric potential are defined in two kinds of regions, walls Γ_w and in/out regions $\Gamma_{i/o}^{i}$ (superscript *i* indicates that there is more than one region of this kind) where the electric potential is applied. In Γ_w boundary conditions are natural,

$$\frac{\partial \phi}{\partial \underline{n}} = 0 \tag{30}$$

where $\underline{n}$ is the outer normal to the surface Γ_w.

In $\Gamma_{i/o}^{i}$ Drichlet conditions were imposed,

$$\phi = \phi_i \tag{31}$$

Solver and preconditioner

To solve this equation conjugate gradient was employed as iterative solver, and an algebraic multigrid preconditioner from PETSc libraries called Boomer AMG.

3.2 Navier – Stokes Equation

Navier – Stokes equation was solved in an incompressible, stationary mode :

$$\underline{\nabla} \cdot (\underline{u}) = 0 \tag{32}$$

$$\rho (\underline{u} \cdot \underline{\nabla} \underline{u}) = -\underline{\nabla} p + \mu \nabla^2 \underline{u} + \rho \underline{g} \tag{33}$$

then is not necessary to set initial conditions nor time stepping settings.

Boundary conditions

In this case a boundary division into two kind of regions is proposed: walls Γ_w and in/out regions $\Gamma_{i/o}^{i}$.

In Γ_w:

$$\underline{u} \cdot \underline{n} = 0 \tag{34}$$

$$\frac{\partial P}{\partial \underline{n}} = 0 \tag{35}$$

$$\underline{u} = \frac{-\zeta \epsilon}{\mu} (\underline{\nabla} \phi_a) \tag{36}$$

where $\underline{n}$ is the outer normal to the surface Γ_w.

In $\Gamma_{i/o}^{i}$:

$$P = P_i \tag{37}$$

$$\frac{\partial \underline{u}}{\partial \underline{n}} = 0 \tag{38}$$

Solver and Preconditioner

To solve this equation an additive Schwartz preconditioner was used , based on domain decomposition method. Two layers of overlapping between subdomains, with maximum size of 2000 elements was employed, and flexible GMRes with restart 300 as iterative solver, in each subdomain, with LU preconditioner.

3.3 Transport equation

Mass transport problem was solved using equation 11.

Initial and Boundary conditions

As in the previous equations two kinds of regions are considered: the reservoir regions Γ_R^i, and rest of boundary surface Γ_w.

Then, in Γ_R^i, Drichlet conditions were imposed for concentration:

$$\text{if } t \geq 0 \Rightarrow c_j = c_0 \tag{39}$$

and, in Γ_w, natural conditions are imposed:

$$\frac{\partial c_j}{\partial \underline{n}} = 0 \tag{40}$$

Solver and Preconditioner

To solve this equation (11) an additive Schwartz preconditioner was used , based on domain decomposition method. Two layers of overlapping between subdomains, with maximum size of 2000 elements was employed, and flexible GMRes with restart 300 as iterative solver, in each subdomain, with LU preconditioner. To improve non linear convergence the Einsenstad-Walker algorithm version 3 (Einsenstad et al., 1996) was used.

Time stepping

In order to develop temporal discretization general scheme was used:

$$t^s = t_{n-1} + \theta t_n \tag{41}$$

with $\theta = 0.55$.

3.4 Hardware

Simulations were carried out using a Beowulf cluster named “Aquiles” at CIMEC (UNL-CONICET), Argentina. “Aquiles” consists in 82 nodes without hard disks, processors Intel Pentium 4 Prescott 3.0GHz 2Mb cache, RAM 2GB DDR 400MHz, LAN cards 3Com 2000ct Gigabit, interconnected by two switches 3Com SuperStack 3 3870 48-ports Gigabit Ethernet.

4 ILLUSTRATION EXAMPLE

In this section, the capability of the model to solve a capillary zone electrophoresis (CZE) in a single capillary is shown. Different levels of approximation in solving electric potential and chemistry are studied.

First potential with Laplace's equation (equation (5)), and without considering any chemical reaction was solved. Then equation (10) was used in order to solve potential without reactions, and finally the complete model was considered, taking into account chemical reactions and

local potential distortions due to the presense of charged species.

4.1 Problem description

The separation process of two analytes, Benzoic Acid and Chlorobenzoic acid, migrating in a buffer of sodium acetate was investigated. A portion of an square (100 μm x 100 μm) section capillary was considered . In order to reduce the domain geometry, an electroosmotic velocity opposed to the migration direction was proposed, in order to preserve the analytes at the center of the channel.

4.2 Physics constants and species properties

In order to solve the problem the physics constants reported in Table 1 were employed.

Symbol	Value	Units	Description
T	300	ºK	Absolute temperature.
ϵ	7.08 e-10	$C^2 N^{-1} m^{-2}$	Water absolute permittivity
F	96485.34	$C\ mol^{-1}$	Faraday constant
k_B	1.38 e-23	$M^2 kg\ s^{-2} K^{-1}$	Boltzmann constant
ρ	1000	$Kg\ m^{-3}$	Water density
μ	0.001	$N\ m^{-2} s^{-1}$	Water dynamic viscosity

Table 1: Physics constants.

Diffusion coefficients and mobilities used for each specie are given in Table 2.

Specie	Valence z_i	Diffusion coefficient D_i (10^{-9} $m^2 s^{-1}$)	Mobility Ω_i (10^{-8} $m^2 V^{-1} s^{-1}$)
Na^+	+1	1.34	5.19
AcO^-	-1	1.08	4.23
Bz^-	-1	0.86	3.36
$BzCl^-$	-1	0.88	3.42
H^+	+1	2.66	10.30
AcOH	-	1.08	-
BzH	-	0.86	-
BzClH	-	0.88	-

Table 2: Species valences, diffusion coefficients and mobilities.

Acidic dissociation constants for buffer and analytes are given in Table 3.

Acid	pK_a	K_a (mol m^{-3})
AcOH	4.76	0.0174
HBz	4.21	0.0616
HBzCl	2.94	1.1481

Table 3: Acidic dissociation constants for buffer and analytes.

4.3 Initial and boundary conditions

For analytes, as initial conditions, identical normal distributions at the center of the channel, were considered as shown for Bz^- in Figure 1. Natural conditions were imposed for all species at the inlets and outlets of the channel. Potential applied was 80 V between channels ends, an equivalent electrokinetic potential $\zeta = 0.035$ V was considered.

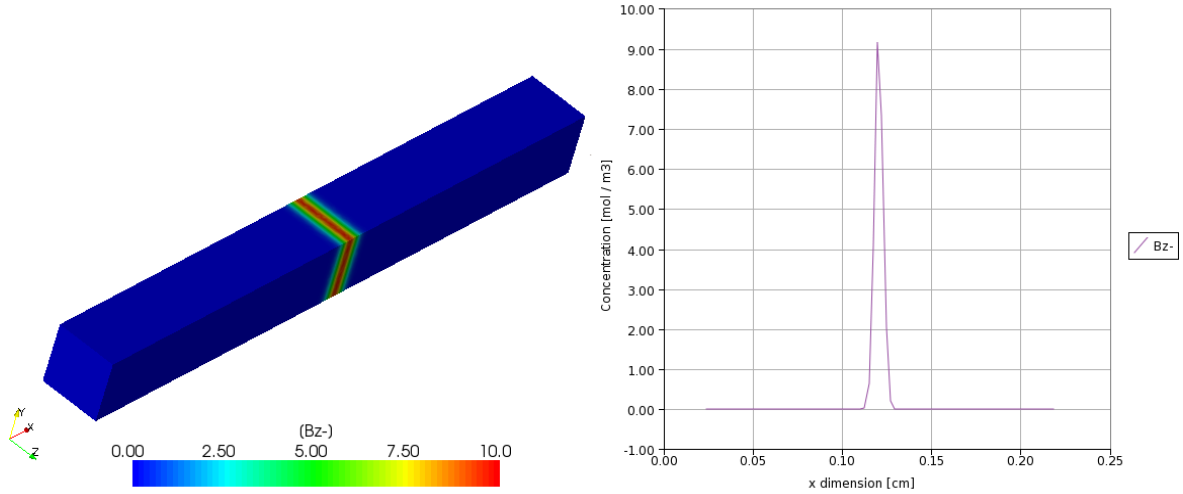

Figure 1: Initial concentration distributions for analytes in mol/m^3.

For buffer components initial constant compositions in whole domain were considered . For the sodium acetate 50 mol m-3 was proposed and, for H+ 0.0631 mol m-3 (pH=4.2).

4.4 Results

Figure 2 shows the concentration fields for Acetic acid, obtained with different approximations in the model. Local variations of electric field (represented correctly by equation 10) produce variations on local concentrations of buffer constituents, which explains system eigenpeaks in CZE (Lopez-Avila et al., 2003).

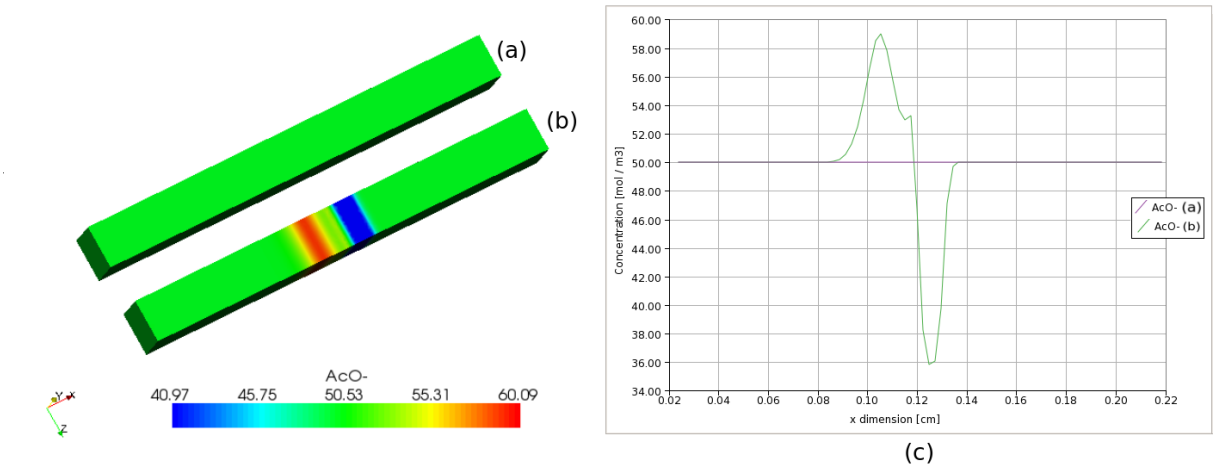

Figure 2: Concentration fields for Acetic acid at t=0.2 s. (a) Solved with equation 5; (b) Solved with equation 10; (c) Both solutions in an 1D plot.

At pH=4.2, half of the total concentration of Benzoic acid is in the acidic form and the other half is in the basic form. In contrast, Chlorobenzoic acid is mostly in its basic form. Therefore at pH=4.2, the migration velocity for Chlorobenzoic acid is larger than the one for Benzoic acid, and consequently the separation efficiency increases. Without including reactions, the analytes are considered as strong electrolytes, this is, they are completely dissociated. This situation occurs at high pH, and is illustrated by Figures 3 to 6, which show concentrations fields for analytes at different pH and running times. Both analytes are in the same cappilary, they are plotted separately for the sake of clarity.

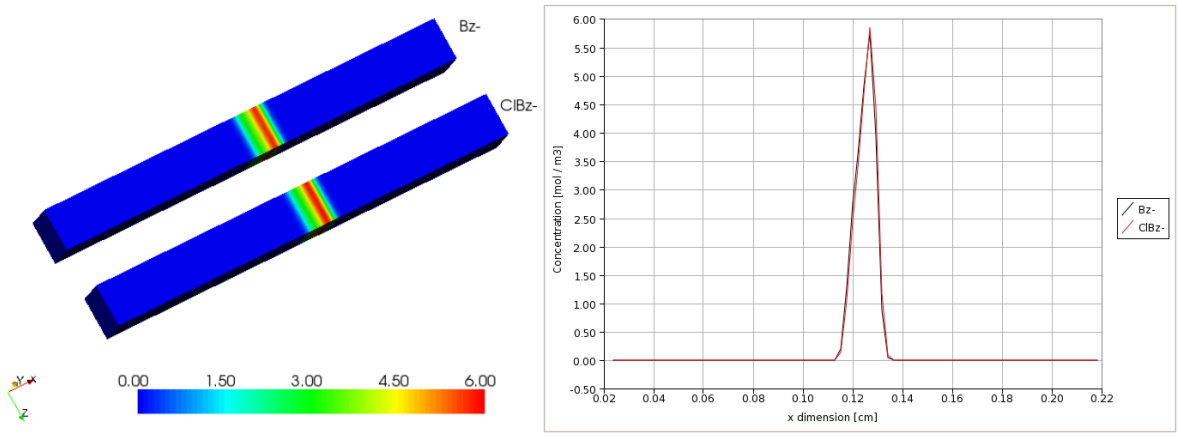

Figure 3: Concentration fields for Bz^- and $BzCl^-$ at pH=7, for t=0.125 s.

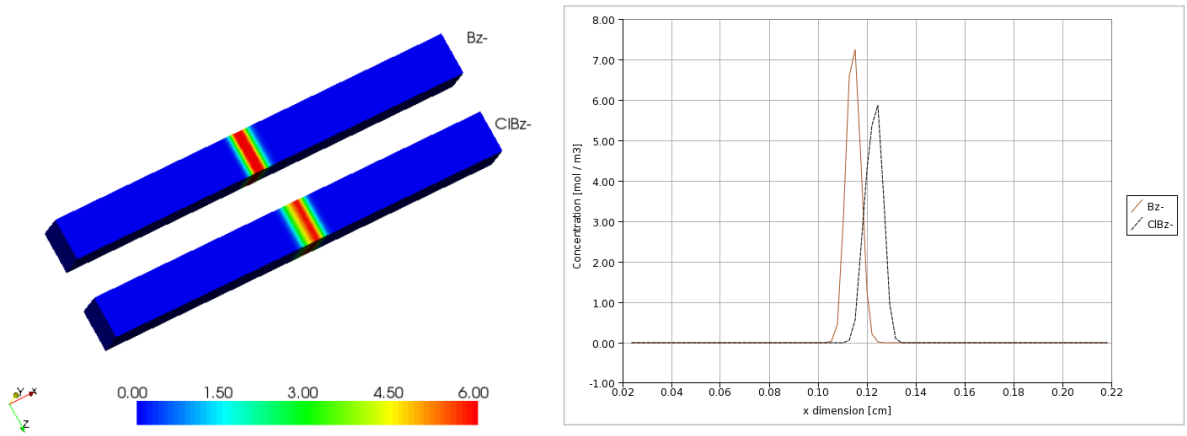

Figure 4: Concentration fields for Bz- and BzCl- at pH=4.2, for t=0.125 s.

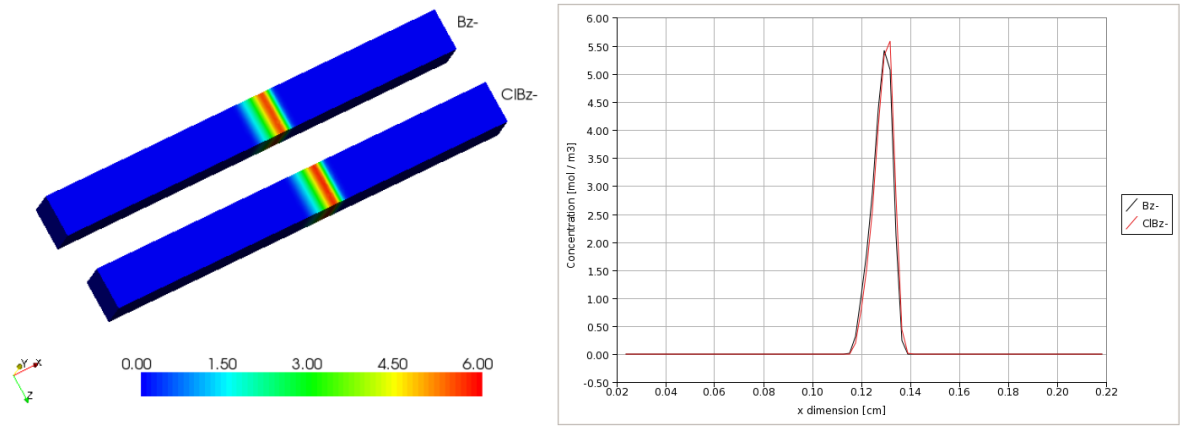

Figure 5: Concentration fields for Bz- and BzCl- at pH=7, for t=0.25 s.

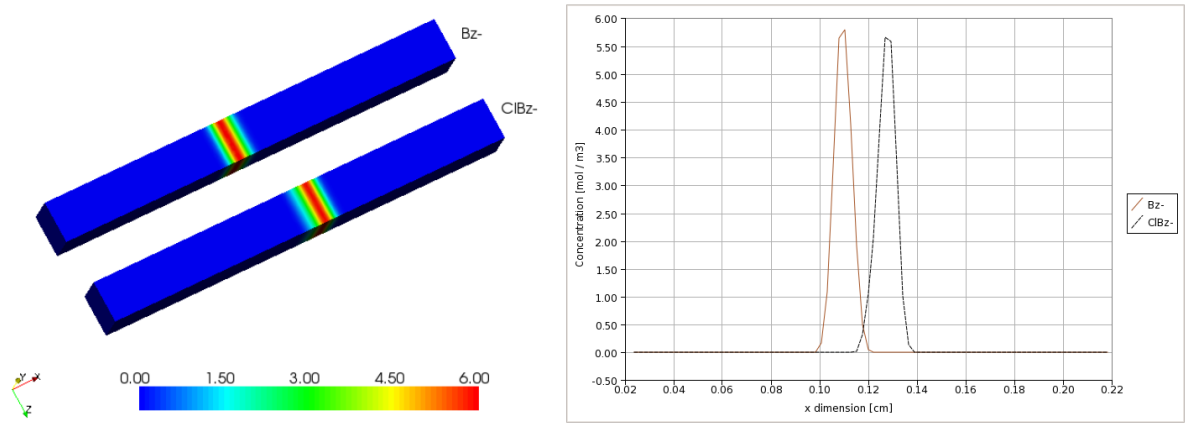

Figure 6: Concentration fields for Bz- and BzCl- at pH=4.2, for t=0.25 s.

5 CONCLUSIONS

The formulation of a generalized numerical model for electrophoretic process was presented, which results suitable for simulation of microfluidcs chips.

A set of equations that governs electrical phenomena, fluids dynamics, mass transport and

chemical reactions was solved, covering different techniques such as CZE. The model allows to simulate processes involving multiple analytes and complex electrolytes buffers. The importance of chemical reactions in this simulations was shown. An example of interest involving electrophoresis on chips was considered as study case.

Numerical simulations were carried out by using high performance parallel computing and solving techniques based on domain decomposition methods. This allows the model be an important tool to design and develop electrophoretic microchips.

ACKNOWLEDGEMENTS

The authors thank Agencia Nacional de Promoción Científica y Tecnológica (ANPCyT) and Consejo Nacional de Investigaciones Científicas y Técnicas (CONICET), Argentina, for the financial aid received.

REFERENCES

Arnaud, I., Josserand, J., Rossier, J., Girault, H., Finite element simulation of Off-Gel^{tm} buffering, *Electrophoresis*, 23: 3253-3261, 2002.

Barz, D., Ehrhard P., Fully coupled modelling of electrokinetic flow and migration of electrolytes in microfluicid devices. *Proceedings of 5th International Conference on Nanochannels, Microchannels and Minichannels*, 2007.

Dalcín, L., Paz, R., Storti., M., MPI for Python: performance improvements and MPI-2 extensions, *Journal of Parallel and Distributed Computing*, 68 (5):665-662, 2008.

Berli, C., Piaggio, M., Deiber, J., Modeling the zeta potential of silica capillaries in relation to the background electrolyte composition, *Electrophoresis*, 24: 1587-1595, 2003.

F. Bianchi, R. Ferrigno, H. H. Girault. Finite element simulation of an electroosmotic-driven flow division at a T-junction of microscale dimensions. *Anal. Chem.*, 72:1987-1993, 2000.

Chatterjee, A., Generalized numerical formulations for multi-physics microfluidics-type applications, *J. Micromech. Microeng.*, 13:758-767, 2003.

Einsenstad, S., Walker, H., Choosing the forcing terms in an inexact Newton method, *SIAM J. Sci. Comput.*,17:16-32,1996.

Erickson, D., Towards numerical prototyping of labs-on-chip: modeling for integrated microfluidic devices. *Microfluid Nanofluid*, 1 (4) :301-318, 2005.

Ermakov, S., Jacobson, S., Ramsey, J., Computer simulations of electrokinetic transport in microfabricated channel structures. *Anal. Chem.*, 70:4494-4504, 1998.

Ermakov, S., Jacobson, S., Ramsey, J., Computer simulations of electrokinetic injection techniques in microfluidic devices. *Anal. Chem.*, 72**:**3512-3517, 2000.

Hunter, R., Foundations of colloid science, Oxford University Press, 1992.

Kirby, B., Hasselbrink Jr, E., Zeta potential of microfluidic substrates: 1. Theory, experimental techniques, and effects on separations, *Electrophoresis*, 25: 187-202, 2004.

Kler, P., Guarnieri, F., Berli, C., Numerical Simulation Of Electrokinetic Flow In Microfluidic Chips, *Mecánica Computacional*, 25:2573-2583, 2006.

Kler, P., Guarnieri, F., Dalcín, L., Modelo numérico eficiente para flujo electrocinético en sistemas microfluídicos con geometrías complejas, *Mecánica Computacional*, 26:485-497, 2007.

Koch, M., Evans, A., Brunnschweiler, A., Microfluidic technology and applications, Research Studies Press Philadelphia, 2000.

Li, D., Electrokinetics in Microfluidcs, Elsevier, 2004.

Lopez-Avila, V., van de Goor, T., Gas B., Coufal, P., Separation of haloacetic acids in water by capillary zone electrophoresis with direct UV detection and contactless conductivity detection, *Journal of Chromatography A*, 993:143-152, 2003.

Manz, A., Graber,N., Widmer, H., Miniaturized Total Chemical Analysis Systems: A novel concept for chemical sensing, *Sens. Actuators B*, 1:244-248 ,1990.

Palusinski, O., Graham, A., Mosher, R., Bier, M., Saville, D., Theory of Electrophoretic Separations. Part II: Construction of a numerical Scheme and its applications, *AICHE Journal*, 32 (2): 215- 223, 1986.

Patankar, N., Hu, H., Numerical simulation of Electroosmotic flow, *Analitical Chemistry*, 70:1870-1881, 1998.

Probstein, R., Physicochemical hydrodynamics, Butterworths, 1989.

Reyes, D., Iossifidis, D., Auroux, P., Manz, A., Micro Total Analysis Systems. 1. Introduction, Theory, and Technology, *Anal. Chem.*, 74: 2623-2636, 2002.

Saville, D., Palusinski, O., Theory of Electrophoretic Separations. Part I: Formulation of a mathematical model , *AICHE Journal*, 32 (2): 207- 214, 1986.